A Chaos-Based Data Gathering Scheme Using Chaotic Oscillator Networks

Hidehiro Nakano, Akihide Utani, Arata Miyauchi and Hisao Yamamoto
Tokyo City University
Japan

1. Introduction

Recently, wireless sensor networks have been studied extensively with a great amount of interest. In wireless sensor networks, many wireless sensor nodes are deployed in an observation area, and monitor status information such as temperature around them. Sensing information is transmitted to and gathered by one or more sink nodes. Each wireless sensor node not only transmits own sensing data but also relays the sensing data from the other wireless sensor nodes. By such a multi-hop wireless communication, the wireless sensor networks are available to observation for large-scale area, and have various applications including natural environmental monitoring. Since wireless sensor nodes generally operate by batteries, efficient data gathering schemes with saving energy consumption of each wireless sensor node are needed for prolonging wireless sensor network lifetime. Ant-based algorithms (Caro et al., 2004; Marwaha et al., 2002; Ohtaki et al., 2006; Subramanian et al., 1998) and cluster-based algorithms (Dasgupta et al., 2003; Heinzelman et al., 2000) have been proposed as routing algorithms. They are more scalable, efficient and robust than the other conventional routing algorithms (Clausen & Jaquet, 2003; Johnson et al., 2003; Ogier et al., 2003; Perkins & Royer, 1999). Sink node allocation schemes based on particle swarm optimization algorithms (Kumamoto et al., 2009; Yoshimura et al., 2009) aim to minimize total hop counts in wireless sensor networks and to reduce energy consumption in each wireless sensor node. Forwarding node set selection schemes (Nagashima et al., 2009; Sasaki et al., 2009) can significantly reduce the number of transmissions of duplicate query messages as compared with original flooding schemes. Secure communication schemes considering energy savings (Li et al., 2009; Wang et al., 2009) have also been proposed. Common purpose of these studies is to prolong wireless sensor network lifetime by saving energy consumption of each wireless sensor node.

Along this line, this study focuses on control schemes for timings of transmissions and receptions of sensing data, proposed as a synchronization-based data gathering scheme (Wakamiya & Murata, 2005). In this scheme, each wireless sensor node has a timer characterized by an integrate-and-fire neuron (Keener et al., 1981). Coupling the timers of wireless sensor nodes which can directly communicate to each other, they construct a pulse-coupled neural network. It is known that pulse-coupled neural networks can exhibit various synchronous and asynchronous phenomena (Catsigeras & Budelli, 1992; Mirollo & Strogatz, 1990). The conventional synchronization-based data gathering scheme is based on the synchronization in pulse-coupled neural networks. As synchronization is achieved, the following control for timings of transmissions and receptions of sensing data is possible: wireless sensor nodes turn

off their power supplies when they do not transmit and receive sensing data. Hence, long-term observation to target area is possible. As a hardware module, a passive wake up scheme for wireless sensor networks has also been proposed (Liang et al, 2008). In the conventional synchronization-based data gathering scheme, it is assumed that wireless sensor nodes do not have any complex routing tables; they transmit and receive sensing data by only referring values of hop counts to the nearest sink node. However, simple pulse-coupled neural networks consisting of integrate-and-fire neurons can exhibit periodic synchronization only. In the conventional synchronization-based data gathering scheme, many duplicate sensing data can be relayed by many wireless sensor nodes. Generally, wireless sensor nodes consume a lot of energy in transmitting sensing data (Heinzelman et al., 2000). Also, in multiple sink wireless sensor networks, multiple sink nodes are allocated on target area, where these are generally distant to each other. If they are not coupled to each other by some communications, it is hard to synchronize all wireless sensor nodes. In order to prolong wireless sensor network lifetime and realize long-term observation, more efficient data gathering schemes are needed.

In the previous works, a chaos-based data gathering scheme has been proposed (Nakano et al., 2009; 2010). In the chaos-based data gathering scheme, each wireless sensor node has a timer characterized by a chaotic spiking oscillator which generates spike-trains with chaotic inter-spike intervals (Nakano & Saito, 2002; 2004). Coupling multiple chaotic spiking oscillators, a chaotic pulse-coupled neural network is constructed. Chaotic pulse-coupled neural networks can exhibit various chaos synchronous phenomena and their breakdown phenomena. The proposed chaos-based data gathering scheme especially applies the breakdown phenomena in chaotic pulse-coupled neural networks. In the phenomena, all chaotic spiking oscillators do not exhibit perfect synchronization. However, partial synchronization on network space and intermittent synchronization on time-domain can be observed depending on parameters. The partial and intermittent synchronization can significantly reduce the redundant transmissions and receptions of sensing data. In the method presented in (Nakano et al., 2009), sensing data is transmitted in the timings when transmitting wireless sensor nodes generate spike signals. In this case, lost sensing data may appear. But, it is confirmed in the numerical experiments that high delivery ratio for sensing data can be kept. In the method presented in (Nakano et al., 2010), sensing data is transmitted in the timings when transmitting wireless sensor nodes accept the spike signals from the other wireless sensor nodes. In this case, it is guaranteed that all sensing data must be transmitted to sink nodes without lost sensing data. Since all chaotic spiking oscillators do not exhibit perfect synchronization, wake up time of each sensor node becomes longer, compared with the conventional synchronization-based data gathering scheme. This method does not aim to reduce energy consumption by turning off power supply of transceivers. However, the partial and intermittent synchronization in the chaos-based data gathering scheme can significantly reduce the total number of transmissions and receptions of sensing data. It can contribute to prolonging wireless sensor network lifetime. Also, the proposed chaos-based data gathering scheme can flexibly adapt not only single sink wireless sensor networks but also multiple sink wireless sensor networks.

This chapter consists of five sections. In Section 2, the conventional synchronization-based data gathering scheme is introduced, and some assumptions for wireless sensor networks in this research is explained. In Section 3, a model of the proposed chaos-based data gathering scheme is explained, and typical phenomena from a simple master-slave network are presented. Then, a basic mechanism of partial and intermittent synchronization in the proposed chaos-based data gathering scheme is discussed. In Section 4, simulation results for two types of wireless sensor networks, a single sink wireless sensor network and a multiple

sink wireless sensor network, are presented. Through simulation experiments, effectiveness of the proposed chaos-based data gathering scheme is shown, and its development potential is discussed. In Section 5, the overall conclusions of this chapter are given and future problems are discussed.

2. Synchronization-Based Data Gathering Scheme

First, a synchronization-based data gathering scheme presented in (Wakamiya & Murata, 2005) are explained. A wireless sensor network consisting of M wireless sensor nodes and L sink nodes are considered. Each wireless sensor node S_i ($i = 1, \cdots, M$) has a timer which controls timing to transmit and receive sensing data. The timer in S_i is characterized by a phase $\phi_i \in [0, 1]$, an internal state $x_i \in [0, 1]$, a continuous and monotone function f_i, a non-negative integer distance level $l_i > 0$, and an offset time δ_i. If each wireless sensor node does not communicate to each other, dynamics of the timer in S_i is described by the following equation.

$$\frac{d\phi_i(t)}{dt} = \frac{1}{T_i}, \text{ for } \phi_i(t) < 1, \tag{1}$$

$$\phi_i(t^+) = 0, \text{ if } \phi_i(t) = 1, \tag{2}$$

where T_i denotes a period of the timer in S_i. That is, if the phase ϕ_i reaches the threshold 1, S_i is said to fire, and the phase ϕ_i is reset to 0 based on Equation (2), instantaneously. The internal state x_i is determined by the continuous and monotone function $f_i(\phi_i)$ where $f_i(0) = 0$ and $f_i(1) = 1$ are satisfied. The following equation is an example of the function f_i.

$$x_i = f_i(\phi_i) = \frac{1}{b_i} \ln(1 + (e^{b_i} - 1)\phi_i), \tag{3}$$

where $b_i > 0$ is a parameter which controls rapidity to synchronization (Mirollo & Strogatz, 1990). From Equations (1) and (3), increase of the phase ϕ_i causes increase of the internal state x_i. If x_i reaches the threshold 1, x_i is reset to the base state 0, instantaneously.

The couplings between each wireless sensor node are realized by the following manner. Let S_j be one of the neighbor wireless sensor nodes allocated in the radio range of a wireless sensor node S_i. The wireless sensor node S_i has a nonnegative integer distance level l_i characterized by the number of hop counts from the nearest sink node. The wireless sensor node S_i transmits a stimulus signal with the own distance level l_i. If S_j receives the signal from S_i, S_j compares the received distance level l_i with the own distance level l_j. If $l_j > l_i$ is satisfied, S_j is said to be stimulated by S_i, and the phase and internal state of S_j change as follows:

$$x_j(t^+) = B(x_j(t) + \varepsilon_j), \tag{4}$$

$$B(x) = \begin{cases} x, & \text{if } 0 \leq x \leq 1, \\ 0, & \text{if } x < 0, \\ 1, & \text{if } x > 1, \end{cases} \tag{5}$$

$$\phi_j(t^+) = f_j^{-1}(x_j(t^+)), \tag{6}$$

where ε_j denotes a strength of the stimulus. After S_j is stimulated, S_j does not respond to all stimulus signals from the neighbor wireless sensor nodes during an offset time δ_j. That is, each wireless sensor node has a refractory period corresponding to the offset time.
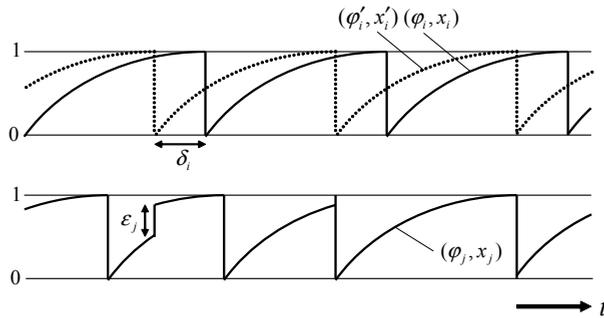
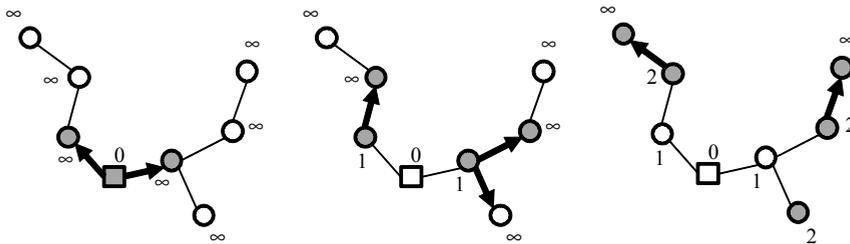Fig. 1. Time-domain waveforms of internal states x_i and x_j ($l_j > l_i$).

Fig. 2. Propagation of stimulus signals and update of distance levels.

The stimulus signals are transmitted by the following manner. A wireless sensor node S_i broadcasts stimulus signals offset time δ_i earlier than the own firing time. That is, S_i broadcasts the stimulus signals if the following virtual internal state x_i' considered the offset time δ_i reaches the threshold 1.

$$\phi_i' = \phi_i + \delta_i \ (\mathrm{mod}\ 1), \tag{7}$$

$$x_i' = f_i(\phi_i'). \tag{8}$$

Fig. 1 shows time-domain waveforms of internal states x_i and x_j, where $l_j > l_i$.
Distance levels of each wireless sensor node are adjusted as shown in Fig. 2. Initially, distance levels of each wireless sensor node are set to sufficiently large values, and that of the sink node is set to 0. A sink node broadcasts "level 0" as a beacon signal. Then, each wireless
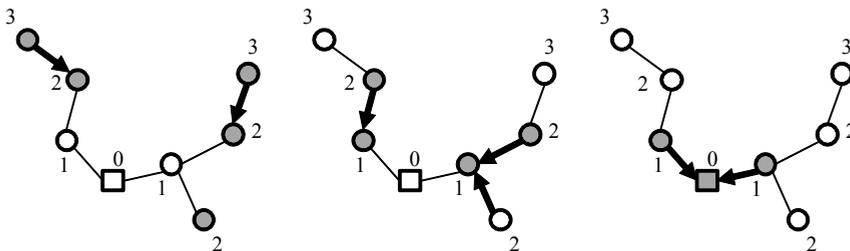

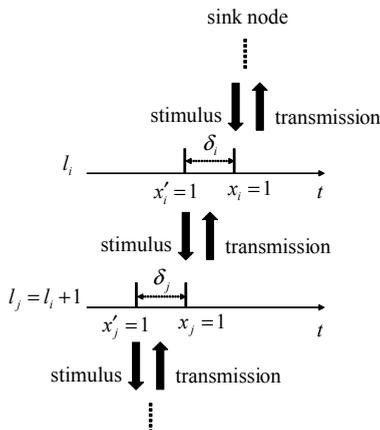Fig. 3. Transmission of sensing data based on distance levels.

Fig. 4. Relaying sensing data ($l_j > l_i$).

sensor node forwards the beacon signal by using flooding, and adjusts each own distance level as corresponding to hop counts to its nearest sink node. The beacon signal is transmitted when each wireless sensor node transmitts stimulus signals. That is, for a stimulus signal from a wireless sensor node S_i, a wireless sensor node S_j adjusts own distance level l_j as follows:

$$l_j = l_i + 1, \text{ if } x'_i(t) = 1 \text{ and } l_j > l_i \tag{9}$$

As a result, each wireless sensor node has a distance level as corresponding to hop counts to its nearest sink node.

Sensing data is transmitted and received as shown in Fig 3. S_i is assumed to receive sensing data from its neighbor wireless sensor node S_j if $l_j = l_i + 1$ is satisfied. Then, S_i aggregate the received sensing data and own sensing data. After that, S_i transmits the aggregated sensing data. Sensing data is assumed to be transmitted and received in each firing period.

The communications between a wireless sensor node S_i and its neighbor wireless sensor node S_j are summarized as follows (see Fig. 4).

- If $l_j = l_i + 1$, S_i receives sensing data from S_j, and aggregates it with the own sensing data. Then, the aggregated sensing data is transmitted to the other wireless sensor nodes.

- If $l_j > l_i$, S_j is stimulated by S_i, and the internal state x_j is changed based on Equation (4). At the same time, the distance level l_j is updated as $l_j = l_i + 1$. After that, S_j does not respond to all stimulus signals during an offset time δ_j.

- Otherwise, both stimulus signals and sensing data are ingored.

As synchronization is achieved by the above explained manner, wireless sensor nodes having large distance levels can transmit sensing data earlier than those having small distance levels. As the offset time is set to sufficiently large value considered conflictions in MAC layer, the sensing data can be relayed sequentially to sink nodes as shown in Fig. 4.

3. Chaos-Based Data Gathering Scheme

In this section, a chaos-based data gathering scheme using a chaotic pulse-coupled neural network presented in (Nakano et al., 2009; 2010) is explained. As same as synchronization-based data gathering scheme, a wireless sensor network consisting of M wireless sensor nodes and L sink nodes are considered. Each wireless sensor node S_i ($i = 1, \cdots, M$) has a timer which controls timing to transmit and receive sensing data. The timer in S_i is characterized by an oscillator having two internal state variables x_i and y_i, a non-negative integer distance level l_i, and an offset time δ_i. Basic dynamics of the timer in S_i is described by the following equation.

$$\frac{d}{dt} \left[\begin{array}{c} x_i(t) \\ y_i(t) \end{array} \right] = \left[\begin{array}{cc} \Delta_i & \omega_i \\ -\omega_i & \Delta_i \end{array} \right] \left[\begin{array}{c} x_i(t) \\ y_i(t) \end{array} \right], \text{ for } x_i(t) < 1 \wedge \bigwedge_j \left(x_j'(t) < 1 \right) \tag{10}$$

$$\left[\begin{array}{c} x_i(t^+) \\ y_i(t^+) \end{array} \right] = \left[\begin{array}{c} q_i \\ y_i(t) - p_i(x_i(t) - q_i) \end{array} \right], \text{ if } x_i(t) = 1 \tag{11}$$

$$\left[\begin{array}{c} x_i(t^+) \\ y_i(t^+) \end{array} \right] = \left[\begin{array}{c} a_i \\ y_i(t) - p_i(x_i(t) - a_i) \end{array} \right], \text{ if } \bigvee_j \left(x_j'(t) = 1 \right) \tag{12}$$

where Δ_i is a damping, ω_i is a self-running angular frequency, p_i is a slope in firing, q_i is a base sate for *self-firing* and a_i is a base state for *compulsory-firing*. j denotes an index of a neighbor wireless sensor node S_j such that $l_j < l_i$. $x_j'(t)$ is a virtual internal state variable of S_j considered an offset time δ_j such that

$$x_j'(t) = x_j(t + \delta_j) \tag{13}$$

If the internal state variable x_i reaches the threshold 1, S_i exhibits *self-firing*, and the internal state (x_i, y_i) is reset to the base state based on Equation (11). If a virtual internal state variable x_j' reaches the threshold 1, S_i exhibits *compulsory-firing*, and the internal state (x_i, y_i) is reset to the base state based on Equation (12). After S_i exhibits *compulsory-firing*, S_i does not exhibit the next *compulsory-firing* during an offset time δ_i. That is, each wireless sensor node has a refractory period corresponding to the offset time. It should be noted that the unit oscillator presented in Section 2 has one internal state variable, and can exhibit periodic phenomena only. The unit oscillator of the proposed chaos-based data gathering scheme has two internal state variables x_i and y_i, and can exhibit various chaotic and bifurcating phenomena (Nakano & Saito, 2002; 2004). Also, it can generate chaotic spike-trains such that series of interspike intervals is chaotic.

Fig. 5 shows a typical chaotic attractor from a unit oscillator without couplings. As $\Delta_i > 0$, the trajectory rotates divergently around the origin. If the trajectory reaches the threshold, it is reset to the base state based on Equation (11). Repeating in this manner, this oscillator exhibits chaotic attractors. Fig. 6 shows typical phenomena from a simple master-slave network consisting of two oscillators, where $M = 2$ and $l_1 < l_2$. As shown in the figure, the first (master) oscillator exhibits chaotic attractors for both $q_i = -0.2$ and $q_i = -0.6$. The second (slave) oscillator is synchronized to the first oscillator for $q_i = -0.2$. That is, the network exhibits master-slave synchronization of chaos. On the other hand, the second oscillator is not perfectly synchronized but intermittently synchronized to the first oscillator for $q_i = -0.6$. These phenomena can be explained by error expansion ratio between the master and slave trajectories (Nakano & Saito, 2002). The case $a_i = 1$ is considered. Let t_n be the n-th *compulsory-firing*
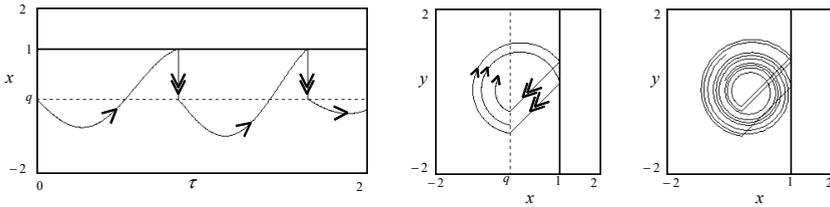
Fig. 5. A typical chaotic attractor from a unit oscillator without couplings. $\Delta_i = 0.25$, $\omega_i = 5$, $p_i = 1$, $q_i = -0.2$.

time of the slave oscillator, let the slave trajectory starts from $(q_i, y_2(t_n^+))$, and let the virtual master trajectory starts from $(q_i, y_1'(t_n^+))$. Let us consider that the $(n + 1)$-th *compulsory-firing* of the slave oscillator occurs at $t = t_{n+1}$ and that each trajectory is reset to each base state. Then, the following average error expansion ratio is defined.

$$\bar{\alpha} \equiv \frac{1}{N} \sum_{n=1}^{N} \ln \alpha_n, \quad \alpha_n \equiv \left| \frac{y_1'(t_{n+1}^+) - y_2(t_{n+1}^+)}{y_1'(t_n^+) - y_2(t_n^+)} \right| \tag{14}$$

If the average error expansion ratio is negative for $N \to \infty$, the slave oscillator is synchronized to the master oscillator as shown in Fig. 6(a). Otherwise, the slave oscillator is not synchronized to the master oscillator. However, depending on sequence $\{\alpha_n\}$, the slave oscillator can be intermittently synchronized to the master oscillator as shown in Fig. 6(b). Such intermittent synchronization plays an important role for effective data gathering by the chaos-based data gathering scheme. Basically, the sequence $\{\alpha_n\}$ is determined by the parameters and initial states of the master and slave oscillators.

Distance levels of each wireless sensor node are adjusted as the the same manners explained in Section 2. Each sink node broadcasts "level 0" as a beacon signal. As each wireless sensor node forwards the beacon signal and adjusts each own distance level, each wireless sensor node has a distance level as corresponding to hop counts to its nearest sink node.

Also, sensing data is transmitted and received as the same manners explained in Section 2. By comparing received distance level with own distance level, sensing data is relayed sequentially to sink nodes. However, chaos-based data gathering scheme can exhibit not only synchronization but also intermittent synchronization. Hence, an assumption as shown in Fig. 7 is additionally introduced. In the figure, stimulus signal is transmitted at $t = t_i'$ from S_i and is received by S_j. Then, S_j broadcasts own sensing data at $t = t_j$. This sensing data can be received by S_i if $t_i' \leq t_j \leq t_i$ and $l_i = l_j - 1$ are satisfied. Each wireless sensor node transmits sensing data to the nearest sink node when stimulus signals are received. Therefore, at least one neighbor wireless sensor node can receive the sensing data even if the chaos-based data gathering scheme exhibits intermittent synchronization.

In wireless sensor networks, energy consumption of transceivers in transmitting sensing data is a dominant factor (Heinzelman et al., 2000). The intermittent synchronization can reduce redundant relays such that the same sensing data is relayed to sink nodes, and can reduce the total number of transmissions in wireless sensor networks. It can contribute to prolonging wireless sensor network lifetime. Also, for effective data gathering, multiple sink nodes should be allocated in an observation area where they are distant from each other (Kumamoto et al., 2009; Yoshimura et al., 2009). If all sink nodes are not coupled to each other via some
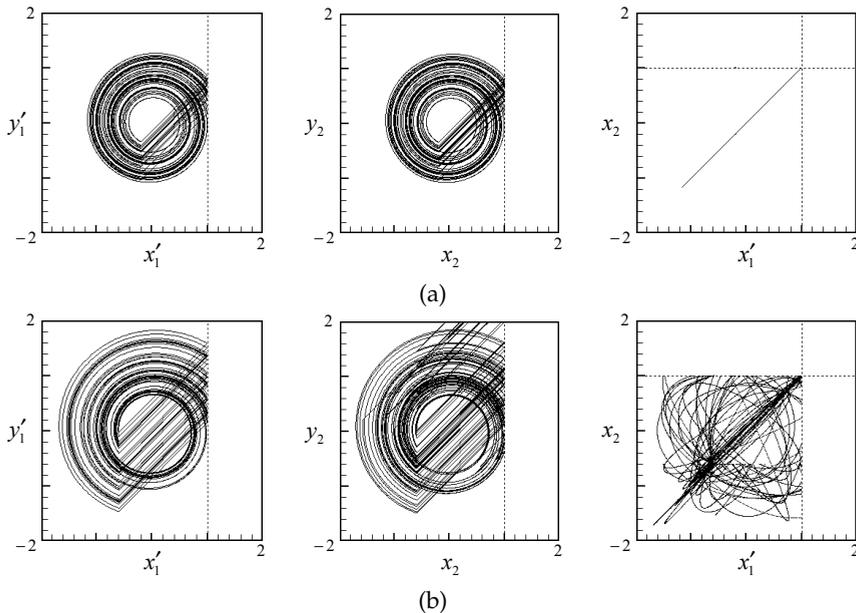
(a)

(b)

Fig. 6. Typical phenomena from a master-slave chaotic pulse-coupled neural network. Left: Master attractors. Center: Slave attractors. Right: Phase relationships. $\Delta_i = 0.25$, $\omega_i = 5$, $p_i = 1$, $a_i = 1$, $\delta_i = 0$ ($i = 1, 2$). (a) Synchronization of chaos: $q_i = -0.2$ ($i = 1, 2$). (b) Intermittent synchronization: $q_i = -0.6$ ($i = 1, 2$).

communications, it is hard to synchronize all wireless sensor nodes. Because, oscillators without couplings never synchronize to each other. The intermittent synchronization can flexibly adapt various wireless sensor networks not only with a single sink node but also with multiple sink nodes. These advantages can be confirmed by the simulation experiments in the next section.

The chaos-based data gathering scheme is based on the conventional synchronization-based data gathering scheme, and does not use any complex protocols using routing tables. Therefore, this method can easily control transmitting and receiving wireless sensor nodes and can flexibly adapt dynamical changes of network topologies. In the conventional synchronization-based data gathering scheme, power supply of transceivers can be turned off when wireless sensor nodes do not transmit or relay sensing data. However, many wireless sensor nodes can relay the same sensing data. The chaos-based data gathering scheme does not aim to reduce energy consumption by turning off power supply of transceivers. However, partial and intermittent synchronization in the chaos-based data gathering scheme can significantly reduce the number of transmitting and receiving sensing data. In addition, this method can guarantee that sensing data from all wireless sensor nodes must be transmitted to sink nodes without loss.
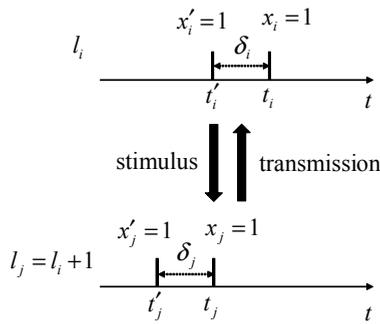
Fig. 7. Relaying sensing data in a chaos-based data gathering scheme ($l_j > l_i$).
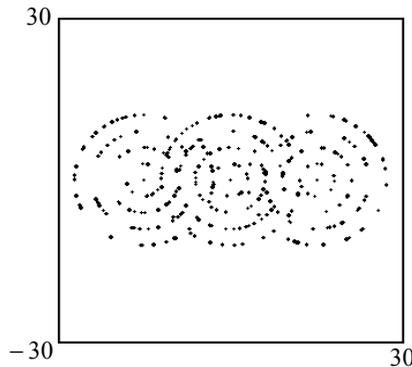

Fig. 8. A model of a wireless sensor network.

4. Numerical Simulations

In order to confirm effectivity of the chaos-based data gathering scheme, numerical simulations are performed. Fig. 8 shows a wireless sensor network model for the simulations. In the figure, 300 wireless sensor nodes are deployed at random locations on 12 concentric circles whose centers are $(-15, 0)$, $(0, 0)$ or $(15, 0)$, and 3 sink nodes are allocated on each center, which is called 3-sink wireless sensor network. On the other hand, in the simulations for 1-sink wireless sensor network, let only a node at $(0, 0)$ be a sink node and let nodes at $(-15, 0)$ and $(15, 0)$ be wireless sensor nodes. The radio range of each wireless sensor node and each sink node is set to 5. The radii of the concentric circles are set to 3, 6, 9 and 12, respectively. $10n$ wireless sensor nodes are set on the n-th concentric circle from each center. Initial values of internal states in each wireless sensor node are set to random values. In the chaos-based data gathering scheme, the parameters are fixed as follows.

$$\forall i, \quad \Delta_i = 0.25, \ \omega_i = 5, \ p_i = 1, \delta_i = 0.2, a_i = 1.$$

Typical simulation results for q_i as a control parameter are shown.
Figs. 9 and 10 show firing time of each wireless sensor node in 1-sink wireless sensor network and 3-sink wireless sensor network, respectively. In the figures, horizontal axis denotes time,
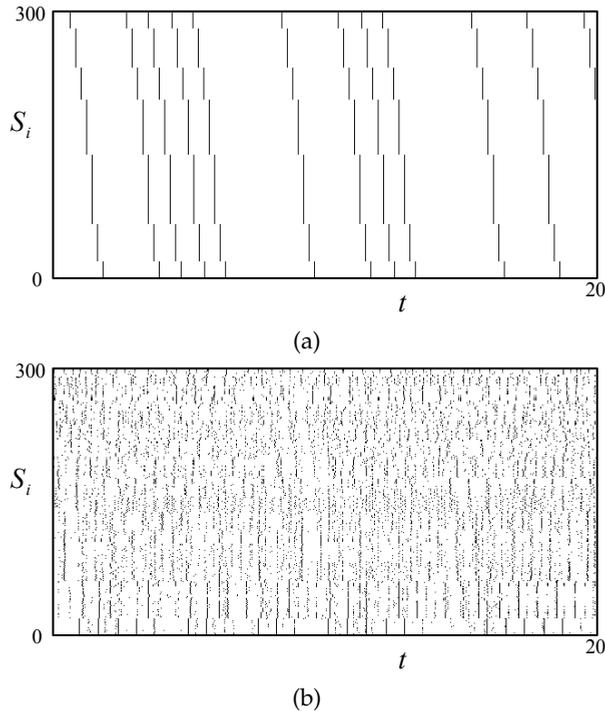
Fig. 9. Firing time of each sensor node in 1-sink wireless sensor network. (a) $q_i = -0.2$. (b) $q_i = -0.6$.

and vertical axis denotes the indexes of each wireless sensor node, where the indexes are sorted by each distance level.

Fig. 9(a) show the results for 1-sink wireless sensor network in $q_i = -0.2$. All internal states are synchronized to each other with time difference depending on their own distance levels. It can also be found that the sequence of the firing time is chaotic. Fig. 9(b) shows the results for 1-sink wireless sensor network in $q_i = -0.6$. All internal states are not synchronized to each other. However, some regularity of firings can be found. Fig. 10(a) shows the results for 3-sink wireless sensor network in $q_i = -0.2$. As compared with Fig. 9(a), chaos synchronization is broken down. It should be noted that it is also hard for the periodic synchronization-based data gathering scheme to synchronize all wireless sensor nodes in the case of multiple sink nodes. Because, frequency and/or phase of each sink node is not synchronized unless each sink node is coupled to each other. Fig. 10(b) shows the results for 3-sink wireless sensor network in $q_i = -0.6$. As compared with Fig. 9(b), significant differences between the cases in a single sink node and in multiple sink nodes can not be found.

Here, wireless sensor nodes which relay sensing data to sink nodes are considered. If all the wireless sensor nodes are synchronized to each other, all sensing data must be relayed to the sink nodes without lost sensing data. However, it is considered that many wireless sensor nodes relay the same sensing data. This problem becomes more serious if density of wireless sensor nodes increases, and the number of wireless sensor nodes and sink nodes increases.
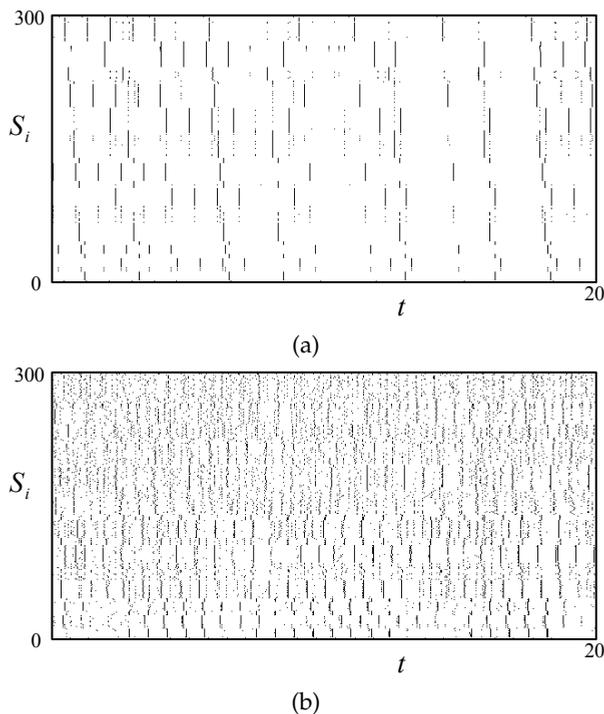
Fig. 10. Firing time of each sensor node in 3-sink wireless sensor network. (a) $q_i = -0.2$. (b) $q_i = -0.6$.

However, it should be noted that sensing data can be relayed to at least one sink node if at least one active path to the sink node exists, although a part of broken paths due to asynchronous firings of transmitting and receiving wireless sensor nodes exists.

In order to evaluate transmission efficiency in more detail, the total number of relays for sensing data from a wireless sensor node to sink nodes are evaluated. 40 wireless sensor nodes S_k ($k = 1, \cdots, 40$) are selected, which are allocated on the most outside of the center concentric circles shown in Fig. 8. S_k transmits sensing data n times. Each sensing data is transmitted in each *compulsory-firing* timing of S_k. It is assumed that only one wireless sensor node in S_k transmits sensing data and the other wireless sensor nodes do not transmit own sensing data. Then, total number of relays for $n = 100$ is calculated.

Figs. 11 and 12 show total number of relays for sensing data in 1-sink wireless sensor network and 3-sink wireless sensor network, respectively. The horizontal axis denotes sorted indexes of the transmitting wireless sensor nodes S_k. The vertical axis denotes the total number of relays, where each value is averaged for the number of transmissions ($n = 100$). The number of relays changes depending on the transmitting wireless sensor nodes. This is due to differences of the number of relay wireless sensor nodes to the sink nodes and/or the number of transmission paths to the sink nodes. That is, this is due to network topology. In the case of 1-sink wireless sensor network and $q_i = -0.2$, all the wireless sensor nodes are synchronized to each other as shown in Fig. 9(a). Then, all sensing data must be transmitted to the sink node without
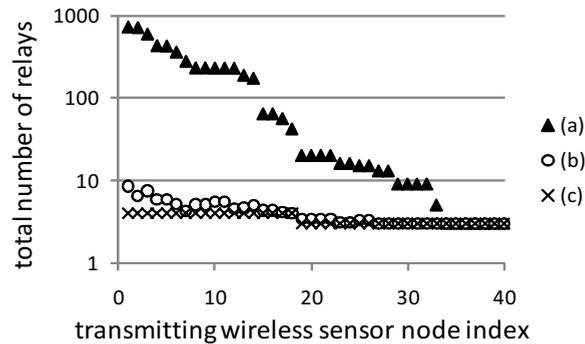
Fig. 11. Total number of relay wireless sensor nodes in 1-sink wireless sensor network. (a) $q_i = -0.2$. (b) $q_i = -0.6$. (c) distance level.
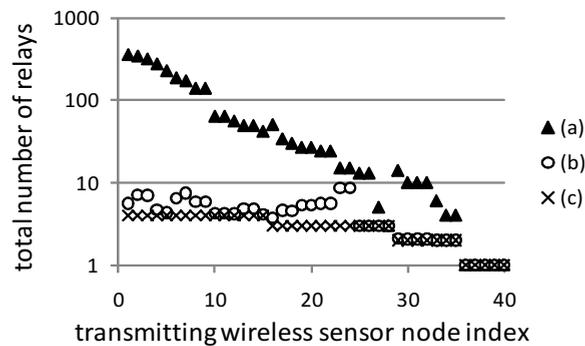

Fig. 12. Total number of relay wireless sensor nodes in 3-sink wireless sensor network. (a) $q_i = -0.2$. (b) $q_i = -0.6$. (c) distance level.

lost sensing data, but the sensing data is relayed by many wireless sensor nodes as shown in Fig. 11(a). In the case of 3-sink wireless sensor network and $q_i = -0.2$, each wireless sensor node is synchronized partially and intermittently to each other as shown in Fig. 10(a). Then, the number of relays for each transmitting wireless sensor node deceases as shown in Fig. 12(a), compared with the case of 1-sink wireless sensor network as shown in Fig. 11(a). In the case of 1-sink wireless sensor network and $q_i = -0.6$, each wireless sensor node is synchronized partially and intermittently as shown in Fig. 9(b). This result is the same also in the case of 3-sink wireless sensor network and $q_i = -0.6$ as shown in Fig. 10(b). Then, the number of relay wireless sensor nodes can be significantly reduced as shown in Figs. 11(b) and 12(b). It can contribute to saving energy consumption of each sensor node. Table 1 shows statistics values of the number of relays for 40 transmitting wireless sensor nodes. These results show that partial and intermittent synchronization can reduce the number of relays. Sensing data can be relayed to a sink node if at least one active path to the sink node exists, although a part of broken paths due to asynchronous firings exists. By the intermittent synchronization in chaos-based data gathering scheme, the number of relays can be significantly reduced. It can contribute to prolonging wireless sensor network lifetime.

	$q_i = -0.2$		$q_i = -0.6$	
	1-sink	3-sink	1-sink	3-sink
average	137.5	71.1	4.1	4.1
maximum	725.0	360.0	8.5	8.6
minimum	3.0	1.0	3.0	1.0

Table 1. Statistics values of number of relays for 40 transmitting wireless sensor nodes.

5. Conclusions

This chapter has analyzed transmission efficiency of a chaos-based data gathering scheme using chaotic pulse-coupled neural networks. Through numerical simulations, it has been shown that this scheme can reduce the total number of wireless sensor nodes which relay the same sensing data, without lost sensing data. For prolonging the lifetime of wireless sensor networks, it is important that the number of transmissions is reduced. In addition, this scheme can be easily applied to wireless sensor networks with multiple sink nodes and shows great performances in the viewpoints of prolonging the lifetime of wireless sensor networks.

Future problems include evaluation of energy consumption and comparison with periodic synchronization-based data gathering schemes in more detail.

6. References

Caro, G.D.; Ducatelle, F. & Gambardella, L.M. (2004). AntHocNet: An ant-based hybrid routing algorithm for mobile ad hoc networks, *Proceedings of 8th International Conference on Parallel Problem Solving from Nature*, 461–470.

Catsigeras, E. & Budelli, R. (1992). Limit cycles of a bineuronal network model, *Physica D*, Vol. 56, 235–252

Clausen, T. & Jaquet, P. (2003). Optimized link state routing protocol, *Request for Comments 3626*

Dasgupta, K.; Kalpakis, K. & Namjoshi, P. (2003). An efficient clustering-based heuristic for data gathering and aggregation in sensor networks, *Proceedings of IEEE Wireless Communications and Networking Conference*, 16–20

Heinzelman, W.R.; Chandrakasan, A. & Balakrishnan, H. (2000). Energy-efficient communication protocol for wireless microsensor networks, *Proceedings of Hawaii International Conference on System Sciences*, 3005–3014

Johnson, D.B.; Maltz, D.A.; Hu, Y.C. & Jetcheva, J.G. (2003). The dynamic source routing protocol for mobile ad hoc networks, *IETF Internet Draft*, draft-ietf-manet-dsr-09.txt

Keener, J.P.; Hoppensteadt, F.C. & Rinzel, J. (1981). Integrate-and-fire models of nerve membrane response to oscillatory input, *SIAM J. Appl. Math.*, Vol. 41, 503–517

Kumamoto, A.; Utani, A. & Yamamoto, H. (2009). Advanced Particle Swarm Optimization for Computing Plural Acceptable Solutions, *International Journal of Innovative Computing, Information and Control*, Vol. 5, No. 11(B), 4383–4392

Li, C.; Hwang, M. & Chu, Y. (2009). An Efficient Sensor-to-sensor Authenticated Path-key Establishment Scheme for Secure Communications in Wireless Sensor Networks, *International Journal of Innovative Computing, Information and Control*, Vol. 5, No. 8, 2107–2124

Liang, S.; Tang, Y. & Zhu, Q. (2008). Passive Wake-up Scheme for Wireless Sensor Networks, *ICIC Express Letters*, Vol. 2, No. 2, 149–154

Marwaha, S.; Tham, C.K. & Srinivasan, D. (2002). A novel routing protocol using mobile agents and reactive route discovery for ad hoc wireless networks, *Proceedings of IEEE International Conference on Networks*, 311–316

Mirollo, R.E. & Strogatz, S.H. (1990). Synchronization of pulse-coupled biological oscillators, *SIAM J. Appl. Math.*, Vol. 50, 1645–1662

Nagashima, J.; Utani, A. & Yamamoto, H. (2009). Efficient Flooding Method Using Discrete Particle Swarm Optimization for Long-Term Operation of Sensor Networks, *ICIC Express Letters*, Vol. 3, No. 3(B), 833–840

Nakano, H. & Saito, T. (2002). Basic dynamics from a pulse-coupled network of autonomous integrate-and-fire chaotic circuits, *IEEE Transactions on Neural Networks*, Vol. 13, No. 1, 92–100

Nakano, H. & Saito, T. (2004). Grouping Synchronization in a Pulse-Coupled Network of Chaotic Spiking Oscillators, *IEEE Transactions on Neural Networks*, Vol. 15, No. 5, 1018–1026

Nakano, H.; Utani, A.; Miyauchi, A. & Yamamoto, H. (2009). Data Gathering Scheme Using Chaotic Pulse-Coupled Neural Networks for Wireless Sensor Networks. *IEICE Transactions on Fundamentals*, Vol. E92-A, No. 2, 459–466

Nakano, H.; Utani, A.; Miyauchi, A. & Yamamoto, H. (2010). Prolonging Lifetime of Multiple-Sink Wireless Sensor Networks Using Chaos-Based Data Gathering Scheme, *Proceedings of ICUFN*, 12–16

Ogier, R.; Lewis, M. & Templin, F. (2003). Topology dissemination based on reverse-path forwarding (TBRPF), *IETF Internet Draft*, draft-ietf-manet-tbrpf-10.txt

Ohtaki, Y.; Wakamiya, N.; Murata, M. & Imase, M. (2006). Scalable and efficient ant-based routing algorithm for ad-hoc networks, *IEICE Transactions on Communications*, Vol. E89-B, No. 4, 1231–1238

Perkins, C.E. & Royer, E.M. (1999). Ad hoc on-demand distance vector routing, *Proceedings of 2nd IEEE Workshop on Mobile Computing Systems and Applications*, 90–100

Sasaki, T.; Nakano, H.; Utani, A.; Miyauchi, A. & Yamamoto, H. (2009). An Efficient Flooding Scheme Using Chaotic Neural Networks in Wireless Sensor Networks, *Proceedings of NOLTA*, 523–526

Subramanian, D.; Druschel, P. & Chen, J. (1998). Ants and reinforcement learning: A case study in routing in dynamic networks, *Technical Report TR96-259*, Rice University

Wakamiya, N. & Murata, M. (2005). synchronization-based data gathering scheme for sensor networks, *IEICE Trans Commun*, Vol. E88-B, No. 3, 873–881

Wang, C.; Hong, T.; Horng, G. & Wang, W. (2009). A GA-based Key-management Scheme in Hierarchical Wireless Sensor Networks, *International Journal of Innovative Computing, Information and Control*, Vol. 5, No. 12(A), 4693–4702

Yoshimura, M.; Nakano, H.; Utani, A.; Miyauchi A. & Yamamoto, H. (2009). An Effective Allocation Scheme for Sink Nodes in Wireless Sensor Networks Using Suppression PSO, *ICIC Express Letters*, Vol. 3, No. 3(A), 519–524
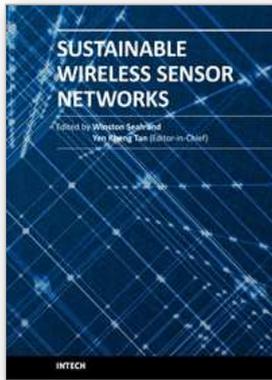
Sustainable Wireless Sensor Networks

Edited by Yen Kheng Tan

Wireless Sensor Networks came into prominence around the start of this millennium motivated by the omnipresent scenario of small-sized sensors with limited power deployed in large numbers over an area to monitor different phenomenon. The sole motivation of a large portion of research efforts has been to maximize the lifetime of the network, where network lifetime is typically measured from the instant of deployment to the point when one of the nodes has expended its limited power source and becomes in-operational â€“ commonly referred as first node failure. Over the years, research has increasingly adopted ideas from wireless communications as well as embedded systems development in order to move this technology closer to realistic deployment scenarios. In such a rich research area as wireless sensor networks, it is difficult if not impossible to provide a comprehensive coverage of all relevant aspects. In this book, we hope to give the reader with a snapshot of some aspects of wireless sensor networks research that provides both a high level overview as well as detailed discussion on specific areas.

How to reference

In order to correctly reference this scholarly work, feel free to copy and paste the following:

Akihide Utani, Arata Miyauchi, Hisao Yamamoto and Hidehiro Nakano (2010). A Chaos-Based Data Gathering Scheme Using Chaotic Oscillator Networks, Sustainable Wireless Sensor Networks, Yen Kheng Tan (Ed.), ISBN: 978-953-307-297-5, InTech, Available from: http://www.intechopen.com/books/sustainable-wireless-sensor-networks/a-chaos-based-data-gathering-scheme-using-chaotic-oscillator-networks

INTECH
open science | open minds